Strange fireball as an explanation of the muon excess in Auger data

Luis A. Anchordoqui,[1,2,3] Haim Goldberg,[4] and Thomas J. Weiler[5]
[1]*Department of Physics and Astronomy, Lehman College, City University of New York, New York 10468, USA*
[2]*Department of Physics, Graduate Center, City University of New York, New York 10016, USA*
[3]*Department of Astrophysics, American Museum of Natural History, New York 10024, USA*
[4]*Department of Physics, Northeastern University, Boston, Massachusetts 02115, USA*
[5]*Department of Physics and Astronomy, Vanderbilt University, Nashville, Tennessee 37235, USA*
(Received 29 December 2016; published 6 March 2017)

We argue that ultrahigh-energy cosmic-ray collisions in Earth's atmosphere can probe the strange quark density of the nucleon. These collisions have center-of-mass energies $\gtrsim 10^{4.6} A$ GeV, where $A \geq 14$ is the nuclear baryon number. We hypothesize the formation of a deconfined thermal fireball which undergoes a sudden hadronization. At production the fireball has a very high matter density and consists of gluons and two flavors of light quarks (u, d). Because the fireball is formed in the baryon-rich projectile fragmentation region, the high baryochemical potential damps the production of $u\bar{u}$ and $d\bar{d}$ pairs, resulting in gluon fragmentation mainly into $s\bar{s}$. The strange quarks then become much more abundant and upon hadronization the relative density of strange hadrons is significantly enhanced over that resulting from a hadron gas. Assuming the momentum distribution functions can be approximated by Fermi-Dirac and Bose-Einstein statistics, we estimate a kaon-to-pion ratio of about 3 and expect a similar (total) baryon-to-pion ratio. We show that, if this were the case, the excess of strange hadrons would suppress the fraction of energy which is transferred to decaying π^0's by about 20%, yielding an ∼40% enhancement of the muon content in atmospheric cascades, in agreement with recent data reported by the Pierre Auger Collaboration.

DOI: 10.1103/PhysRevD.95.063005

I. INTRODUCTION

Ultrahigh-energy ($E \gtrsim 10^{9.8}$ GeV) cosmic rays provide a formidable beam to study particle collisions at center-of-mass energies and kinematic regimes not accessible at terrestrial accelerators. The incident cosmic radiation interacts with the atomic nuclei of air molecules and produces air showers which spread out over large areas. If the primary cosmic ray is a baryon, hundreds to thousands of secondary particles are usually produced at the interaction vertex, many of which also have energies above the highest accelerator energies [1]. These secondary products are of course intrinsically hadrons. Generally speaking, by extrapolating final states observed at collider experiments, we can infer that, for pp collisions at center-of-mass energy $\sqrt{s} \sim 140$ TeV, the jet of hadrons contains about 75% pions (including 25% π^0's, in accord with isospin invariance), 15% kaons, and 10% nucleons [2].

During the shower evolution, the hadrons propagate through a medium with an increasing density as the altitude decreases and the hadron-air cross section rises slowly with energy. Therefore, the probability for interacting with air before decay increases with rising energy. Moreover, the relativistic time dilation increases the decay length by a factor E_h/m_h, where E_h and m_h are the energy and mass of the produced hadron. When the π^0's (with a lifetime of $\simeq 8.4 \times 10^{-17}$ s) do decay promptly to two photons, they feed the electromagnetic component of the shower. For other longer-lived mesons, it is instructive to estimate the critical energy at which the chances for interaction and decay are equal. For a vertical transversal of the atmosphere, such a critical energy is found to be $\xi_c^{\pi^\pm} \sim 115$ GeV, $\xi_c^{K^\pm} \sim 850$ GeV, $\xi_c^{K_L^0} \sim 210$ GeV, $\xi_c^{K_S^0} \sim 30$ TeV [3]. The dominant K^+ branching ratios are to $\mu^+\nu_\mu(64\%)$, to $\pi^+\pi^0(21\%)$, to $\pi^+\pi^+\pi^-(6\%)$, and to $\pi^+\pi^0\pi^0(2\%)$, whereas those of the K_S^0 are to $\pi^+\pi^-(60\%)$, to $\pi^0\pi^0(30\%)$, and for K_L^0 we have $\pi^\pm e^\mp \nu_e(40\%)$, $\pi^\pm \mu^\mp \nu_\mu(27\%)$, $\pi^0\pi^0\pi^0(19\%)$, $\pi^+\pi^-\pi^0(12\%)$ [4]. With these figures in mind, to a first approximation it seems reasonable to assume that in each generation of particles about 25% of the energy is transferred to the electromagnetic shower, and all hadrons with energy $\gtrsim \xi_c^{\pi^\pm}$ interact rather than decay, continuing to produce the hadronic shower.[1] Eventually, the electromagnetic cascade dissipates around 90% of the primary particle's energy and the remaining 10% is carried by muons and neutrinos.

As the cascade process develops in the atmosphere, the number of particles in the shower increases until the energy of the secondary particles is degraded to the level where

[1]The electromagnetic shower fraction from pions only is less than 25%, but simulations show that inclusion of other hadronic resonances brings the electromagnetic shower fraction up to about 25% [5]. We take 25% as a reasonable estimate of the energy transfer to the electromagnetic shower.

ionization losses dominate. At this point the density of particles starts to decline. The number of particles as a function of the amount of atmosphere penetrated by the cascade (X in g cm^{-2}) is known as the longitudinal profile. A well-defined peak in the longitudinal development, $X_{\rm max}$, occurs where the number of $e^{\pm}$'s in the electromagnetic shower is at its maximum. $X_{\rm max}$ increases with primary energy, as more cascade generations are required to degrade the secondary particle energies. Evaluating $X_{\rm max}$ is a fundamental part of many of the composition analyses done when studying air showers. The generic shower properties can be qualitatively well understood using the superposition principle, which states that a shower initiated by a nucleus with A nucleons and energy E behaves to a good approximation as the superposition of A proton showers with initial energy E/A [6]. This phenomenological assumption relies on the fact that the effect of nuclear binding must be negligible at extremely high energies. Thus, for a given total energy E, showers initiated by a heavy nucleus have a smaller $X_{\rm max}$ than proton induced showers.

The integrated longitudinal profile provides a calorimetric measurement of the energy of the primary cosmic ray, with a relatively small uncertainty due to the correction for energy lost to neutrinos and particles hitting the ground. The characteristics of the cascade depend dominantly on the elasticity (the fraction of incoming energy carried by the leading secondary particle) and the multiplicity of secondary particles in the early, high-energy interactions. Modeling the development of a cosmic-ray air shower requires extrapolation of hadronic interaction models tuned to accommodate LHC data [7]. Not surprisingly, such extrapolation usually leads to discrepancies between measured and simulated shower properties. The hadronic interaction models are further constrained by independent measurements of $X_{\rm max}$ and the density of muons at 1 km from the shower core N_μ [8]. The mean $X_{\rm max}$ is primarily sensitive to the cross section, elasticity, multiplicity, and primary mass. The mean N_μ is primarily sensitive to the multiplicity, the π^0 energy fraction (the fraction of incident energy carried by π^0's in hadronic interactions), and the primary mass.

Over the past few decades, it has been suspected that the number of registered muons at the surface of Earth is by some tens of percentage points higher than expected with extrapolations of existing hadronic interaction models [9,10].[2] Very recently, a study from the Pierre Auger Collaboration [12] has strengthened this suspicion, using a novel technique to mitigate some of the measurement uncertainties of earlier methods [5]. The new analysis of Auger data suggests that the hadronic component of showers (with primary energy $10^{9.8} < E/{\rm GeV} < 10^{10.2}$) contains about 30% to 60% more muons than expected. The significance of the discrepancy between data and model prediction is somewhat above 2.1σ.

[2]See, however, [11].

Changing the π^0 energy fraction or suppressing π^0 decay are the only modifications which can be used to increase N_μ without coming into conflict with the $X_{\rm max}$ observations [13].[3] Several new physics models have been proposed exploring these two possibilities [13–15]. In this paper we adopt a purely phenomenological approach to develop an alternative scheme. In sharp contrast to previous models, our proposal is based on the assumption that ultrahigh-energy cosmic rays are heavy (or medium mass) nuclei. Our work builds upon some established concepts, yet contravenes others.

We conceive the production and separation of strangeness in a baryon-rich *Centauro-like* fireball before its spontaneous *explosive* decay [16–20]. At production the fireball has a very high matter density and consists of gluons and two flavors of light quarks (u, d). Because the fireball is formed in the baryon-rich projectile fragmentation region, the high baryochemical potential slows down the creation of $u\bar{u}$ and $d\bar{d}$ pairs, resulting in gluon fragmentation dominated by $g \to s\bar{s}$. The larger amount of u and d with respect to $\bar{u}$ and $\bar{d}$ gives a higher probability for $\bar{s}$ to find u or d and form K^+ or K^0 than for s to form the antiparticle counterparts. Prompt *hard* kaon emission then carries away all strange antiquarks and positive charge, lowering somewhat the initial temperature and entropy. The late-stage hadronization is characterized by production of K^-, $\bar{K}^0$, nucleons, pions, and strange baryons. Overall, after hadronization is complete, the relative density of strange hadrons is significantly enhanced over that resulting from a hadron gas alone, damping the π^0 energy fraction.

The layout of the paper is as follows. We begin in Sec. II with an overview of the fireball paradigm and make a critical review of the available experimental data from colliders. After that, in Sec. III we discuss the particulars of air-shower evolution and present our results from Monte Carlo simulations. We show that the formation of a plasma, with gluons and massive quarks, could play a key role in the hadronization process, modifying shower observables. In particular, we demonstrate that air showers triggered by a fireball explosion tend to increase N_μ, and under some reasonable assumptions can accommodate Auger data. Finally, we summarize our results and draw our conclusions in Sec. III.

II. FIREBALL PHENOMENOLOGY

It has long been suspected that, for systems of high energy density, the elementary excitations can be safely

[3]We note in passing that muons may be able to escape the shower core before reaching Earth's surface if their production angle is increased by boosting the p_T distribution. Since the muon lateral distribution function is a steeply falling function of the radius, a larger production angle would increase N_μ. However, as shown in [13], the measured zenith angle dependence of the ground signal vetoes the correlated flattening of the muon lateral distribution function necessary to accommodate Auger data.

approximated by an ensemble of free quarks and gluons at finite temperature and baryon number density [21–23]. This is because when the energy density is extremely high, the expected average particle separation is so small that the effective strength of interactions is weak (asymptotic freedom) [24,25]. For many purposes, the order of the energy density of matter inside a heavy nucleus is immense,

$$\varepsilon_A \sim \frac{m_p A}{\frac{4}{3}\pi R^3} \sim 0.15 \text{ GeV/fm}^3, \tag{1}$$

where m_p is the proton mass, A is the nuclear baryon number, and $R \sim 1.1A^{1/3}$ fm is the nuclear radius. However, at typical energy densities inside of nuclei, quarks and gluons are very probably confined, on the average, inside of hadrons such as protons, neutrons, or pions. For $\varepsilon \gg 0.15$ GeV/fm^3 all of these hadrons could be squeezed so tightly together that on average they will all overlap and the system would become an unconfined plasma of quarks and gluons, which are free to roam the system. The energy scale at which hadrons begin to overlap is above the energy density of matter inside the proton, $\varepsilon_p \sim 0.5$ GeV/fm^3, where we have taken the radius of the proton as measured in electron scattering $R \sim 0.8$ fm. Indeed, using phenomenological considerations it is straightforward to estimate that the critical energy density to form a nonhadronic medium is around 1 GeV/fm^3 [26]. This result is supported by high-statistics lattice-QCD calculations, which yield $\varepsilon_c \sim 7T_c^4 \sim 1$ GeV/fm^3, where we have taken $T_c = 190$ MeV [27].

Besides the early Universe, the conditions of extremely high temperature and density necessary for the appearance of unconfined quark and gluons could occur in at least two other physical phenomena: (i) the interiors of neutron stars [28–34] and (ii) high-energy nucleus-nucleus collisions, whether artificially produced at accelerators or naturally occurring interactions of cosmic rays with particles in Earth's atmosphere [35–38]. We estimate the energy density in nucleus-nucleus collisions of cosmic rays following [26]. We assume there exists a "central-plateau" structure in the inclusive particle productions as a function of the pseudorapidity variable. The energy per particle should be of the order of the typical transverse momentum per particle $\langle p_T \rangle$. More precisely, in the fireball frame each isotropically emitted particle has an energy given by

$$\langle E \rangle \sim [(4\langle p_T \rangle/\pi)^2 + m^2]^{1/2}, \tag{2}$$

where m is the particle's mass [18]. The energy content is approximately $\delta_A \langle E \rangle dN_{\text{ch}}$, where dN_{ch} is the charged-hadron multiplicity per pp collision, and δ_A the number of nucleon-nucleon interactions in the fireball during the collision. Consider two nuclei of transverse radius R which collide in the center-of-mass frame. The longitudinal size of the nuclei is Lorentz contracted forming a transverse thin slab at midpseudorapidity. The initial *fireball* volume is $dV = (R^2\pi)\tau_0 d\eta_0$, where τ_0 is the typical time scale for the formation and decay of a central fireball and hence $\tau_0 d\eta_0$ is the longitudinal size, with $d\eta_0$ being the pseudorapidity width at τ_0. The time scale can be estimated as the time to traverse at light speed the fireball diameter, i.e., $\tau_0 = 2R/c \sim 3 \times 10^{-23}$ s. The energy density during the cosmic-ray (CR) collision is then

$$\varepsilon_{\text{CR}} \sim \delta_A \langle E \rangle \frac{1}{\pi R^2 \tau_0} \left. \frac{dN_h}{d\eta} \right|_{\eta=0}. \tag{3}$$

The average transverse momentum of charged hadrons produced in pp collisions can be parametrized as a function of the squared center-of-mass energy,

$$\langle p_T \rangle = (0.413 - 0.0171 \ln s + 0.00143 \ln^2 s) \text{ GeV}, \tag{4}$$

with s in appropriate units of GeV^2 [39]. On the other hand, for a cosmic-ray nitrogen nucleus (for simplicity, we choose the beam nucleus to be that of the dominant element in air[4]) of $E \approx 10^{10}$ GeV colliding with an air nucleus, we have $\sqrt{s} \approx 10^{4.6} A$ GeV, yielding $\langle p_T \rangle \sim 0.69$ GeV and $(dN_{\text{ch}}/d\eta)_{\eta=0} \sim 7$ [40]. Throughout, we take $A = 14$ as fiducial in our calculations and assume that half of this number of nucleons interact per collision, producing the fireball. Therefore, taking an effective mass $m \sim 500$ MeV and $\delta_A = A/2$, the energy density in such a scattering process is

$$\varepsilon_{\text{CR}} \sim 2.2 \text{ GeV/fm}^3, \tag{5}$$

well above ε_c, complying with the requirement for the formation of a deconfined thermal fireball.

We envision the fireball as a plasma of *massive* quarks and gluons maintained in both kinetic and chemical equilibrium. Because the total number of particles is allowed to fluctuate, we adopt the viewpoint of the grand canonical ensemble. In this representation, which allows an exchange of particles among the system and the reservoir, the control variables are the baryochemical potential μ_B and the temperature T. In the limit $\mu_B \to 0$ and $T \to 0$ the system becomes the vacuum.

The momentum distribution functions $f(p)$ can be approximated by Fermi-Dirac (+) and Bose-Einstein (−) statistics,

[4]In air, nitrogen is a dimer, N_2, with total $A = 2 \times 14 = 28$. However, the electronic binding is ∼eV, whereas the nuclear binding is ∼MeV, so the energy scales and length scales differ by $\sim 10^6$, and the dimerization is not expected to survive the cosmic-ray production process. The nuclear binding of the single nucleus apparently does survive this process.

$$f_{i,\pm}(p) = \left[\exp\left(\frac{\sqrt{p^2+m_i^2}-\mu_i}{T}\right) \pm 1\right]^{-1}, \quad (6)$$

yielding the following equilibrium number densities:

$$n_{i,\pm} = g_i \int \frac{d^3p}{(2\pi)^3} f_{i,\pm}(p), \quad (7)$$

where the index i runs over $\{u, d, s, g\}$, $\mu_s = 0$ because of the total strangeness neutrality of the initial state, $\mu_u = \mu_d \equiv \mu_q = \mu_B/3$, p and m_i are the particle's momentum and mass, and g_i is the spin-color degeneracy factor. The plus sign is to be used for quarks and the minus sign for gluons, with $\mu_g = 0$. The density of the strange quarks is found to be (two spins and three colors)

$$\begin{aligned} n_s = n_{\bar{s}} &= 6\int \frac{d^3p}{(2\pi)^3}\frac{1}{e^{\sqrt{p^2+m_s^2}/T}+1} \\ &= \frac{3}{\pi^2}T^3\sum_{n=1}^{\infty}\frac{(-1)^{n+1}}{n^3}(nm_s/T)^2K_2(nm_s/T) \\ &\approx \frac{3}{\pi^2}m_s^2TK_2(m_s/T), \end{aligned} \quad (8)$$

where $K_2(x)$ is the second-order modified Bessel function [41,42]. In addition, there is a certain light antiquark density ($\bar{q}$ stands for either $\bar{u}$ or $\bar{d}$):

$$\begin{aligned} n_{\bar{q}} &= 6\int \frac{d^3p}{(2\pi)^3}\frac{1}{e^{|p|/T+\mu_q/T}+1} \\ &= \frac{6}{\pi^2}T^3\sum_{n=1}^{\infty}\frac{(-1)^{n-1}}{n^3}e^{-n\mu_q/T} \\ &\approx \frac{6}{\pi^2}T^3e^{-\mu_q/T}. \end{aligned} \quad (9)$$

Note that the baryonic chemical potential exponentially suppresses the $q\bar{q}$ pair production. This reflects the chemical equilibrium between $q\bar{q}$ and the presence of a light quark density associated with the net baryon number. Now, since the chemical potentials satisfy $\mu_q = -\mu_{\bar{q}}$, it follows that [43]

$$\begin{aligned} n_q - n_{\bar{q}} &= \frac{g_i}{2\pi^2}\int_0^{\infty} dp\,p^2\left(\frac{1}{e^{(p-\mu_q)/T}+1} - \frac{1}{e^{(p+\mu_q)/T}+1}\right) \\ &= \frac{\mu_q^3}{\pi^2} + \mu_q T^2. \end{aligned} \quad (10)$$

Note that this result is exact and not a truncated series. The gluon density also follows from (7) and is given by

$$n_g = \frac{16}{\pi^2}\zeta(3)T^3, \quad (11)$$

where $\zeta(x)$ is the Riemann function. (See Appendix A for details.) By comparing (8) and (9), it is straightforward to see that there are often more $\bar{s}$'s than antiquarks of each light flavor,

$$\frac{n_{\bar{s}}}{n_{\bar{q}}} \approx \frac{1}{2}\left(\frac{m_s}{T}\right)K_2(m_s/T)e^{\mu_q/T}. \quad (12)$$

For $T \gtrsim m_s$ and $\mu_B \to 0$, there are about as many u and d quarks as there are s quarks.

For $T \gg T_c$, many of the properties of the quark-gluon plasma can be calculated in the framework of thermal perturbation theory. Neglecting quark masses in first-order perturbation theory, the energy density of the *ideal* quark-gluon plasma is found to be

$$\begin{aligned} \varepsilon_{\rm QGP} = &\left[\frac{1}{30}\left(N_g + \frac{7}{4}N_q\right) - \frac{11\alpha_s}{3\pi}\right]\pi^2T^4 + \left(\frac{N_q}{4} - \frac{6\alpha_s}{\pi}\right)\mu_q^2T^2 \\ &+ \left(\frac{N_q}{8} - \frac{3\alpha_s}{\pi}\right)\frac{\mu_q^4}{\pi^2} + B, \end{aligned} \quad (13)$$

where $N_g = 16$ and N_f are the gluon and quark degrees of freedom, α_s is the QCD coupling constant, and B is the difference between the energy density of the perturbative and the nonperturbative QCD vacuum (the bag constant) [44–46]. One observes that (13) is essentially the equation of state of a gas of massless particles with corrections due to QCD perturbative interactions, which are always negative and thus reduce the energy density at a given temperature T.

Since the u and d flavors are almost massless even in the fireball phase, we can get an estimate of the baryochemical potential by considering only the contribution from the nearly massless (even in the fireball phase) two quarks at $T = 0$. For two quark flavors, $N_f = 12$ and so (13) simplifies to

$$\varepsilon_{\rm fb}^{T=0} = \left(\frac{3}{2} - \frac{3\alpha_s}{\pi}\right)\frac{\mu_q^4}{\pi^2} + B. \quad (14)$$

Substituting (5) into (14), with $\alpha_s \simeq 0.2$ [47] and the MIT bag constant $B^{1/4} \approx 328$ MeV [45], we obtain

$$\mu_B \sim 2.0 \text{ GeV}. \quad (15)$$

The temperature of the plasma can be approximated by [43]

$$T = \frac{2}{3}(\langle E\rangle - m) \sim 580 \text{ MeV}. \quad (16)$$

A point worth noting at this juncture is that the shapes of the p_T spectra are expected to be determined by an interplay between two effects: the thermal motion of the particles in the fireball and a pressure-driven radial flow, induced by the fireball expansion. To disentangle the two

contributions, namely thermal motion and transverse flow, one has to rely on model calculations which seem to indicate that the observed temperature in the particle spectra is close if not exactly equal to the temperature value that would be present in the chemically equilibrated fireball [48].

Substituting (15) and (16) into (12), with $m_s \simeq 175$ GeV, we obtain $n_{\bar{s}}/n_{\bar{q}} \sim 3.1$. The pion-to-nucleon density ratio is found to be

$$\frac{n_\pi}{n_N} \sim \varkappa \frac{3}{2} \exp\{[m_N - 4\mu_B/3 - m_\pi]/T\}, \tag{17}$$

where the factor $3/2$ comes from the number of the particle species, m_π is the pion mass, $m_N \sim 1$ GeV is the average baryon mass, and $\varkappa$ is a normalization constant fixed by the choice of boundary values [18].

It is worth commenting on an aspect of this analysis which may seem discrepant at first blush. From relativistic heavy-ion experiments one infers a temperature falling with the chemical potential, from $T(\mu_B = 0) = 166$ MeV. However, to accommodate the muon excess in Auger data one needs $T(\mu_B = 2\ \text{GeV}) = 580$ MeV. Details of this discrepancy and eventual accommodation are given in Appendix B.

In our analysis we will adopt a pragmatic approach and avoid the details of theoretical modeling of the hadronization process. Which of the two points of view one may find more convincing, it seems most conservative at this point to depend on experiments to resolve the issue. The multiplicity ratio $\pi\!:\!K\!:\!N \sim 0.15\!:\!0.45\!:\!0.40$ has been eyeball fitted to reproduce the anomalous muon signal observed in Auger data. We show the success of this protocol in the next section. Here we simply note that these ratios are in partial agreement with (12) and (17) for $\varkappa \sim 7$.

III. AIR-SHOWER EVOLUTION

We now make contact with the shower evolution. As a first-order approximation we adopt a basic phenomenological approach. Namely, we assume that the hadronic shower carries a fraction f_h of the total energy of the primary cosmic ray E, which scales as

$$f_h \sim (1 - f_{\rm EM})^{n_{\rm gen}}, \tag{18}$$

where $n_{\rm gen}$ is the number of generations required for most pions to have energies below $\xi_c^{\pi^\pm}$ and $f_{\rm EM}$ is the average fraction in electromagnetic particles per generation [49]. In the canonical framework hadronic interaction models transfer about 25% of the energy to the electromagnetic shower. Conspicuously, the production of light hadrons in this canonical framework is virtually local in rapidity and, therefore, since the interaction models are tuned to fit collider data, $f_{\rm EM}$ would remain approximately constant with energy. We have found that for the considerations in the present work we can safely approximate that each interaction diverts about 75% of the available energy into pions and 15% into kaons, while 10% continues as nucleons. Roughly speaking, this is consistent with a multiplicity ratio $\pi\!:\!K\!:\!N \simeq 0.75\!:\!0.15\!:\!0.10$. Now, taking then $f_{\rm EM} \sim 0.25$ and $f_h \sim 0.10$ we conclude that $n_{\rm gen} \sim 8$.[5] This is in agreement with the estimates of [49] which indicate that the number of interactions needed to reach $\xi_c^{\pi^\pm}$ is $n_{\rm gen} = 3,\ 4,\ 5,\ 6$ for $E = 10^5,\ 10^6,\ 10^7,\ 10^8$ GeV, respectively.

A comprehensive study of the uncertainties associated with the modeling of hadronic interactions indicates that a simple reduction of $n_{\rm gen}$ to increase f_h correlates with $X_{\rm max}$, which becomes too shallow before N_μ is sufficiently increased to accommodate Auger data [13].

Now, if the shower is initiated in a fireball explosion in the first generation, then we have seen that we can approximate the multiplicity ratios by $\sim 0.15\!:\!0.45\!:\!0.40$. Moreover, this is a completely inelastic process, but differs from the usual inelastic processes in that a fireball is also produced. We assume this fireball creates a higher multiplicity of particles and to a first approximation equally partitions energy among the secondaries (thereby negating a large leading particle effect). The fireball production thus accelerates the cooling of the cascade and could reduce the number of generations. We denote by $n'_{\rm gen}$ the numbers of generations for a shower initiated by a fireball. We may then assume that $n'_{\rm gen} \sim 7$ or 8 would be enough to reach the critical shower energy $\xi_c^{\pi^\pm}$. To include the fireball effects we rewrite (18) as

$$f_h \sim (1 - f_{\rm EM}^{\rm fb})(1 - f_{\rm EM})^{n'_{\rm gen}-1}, \tag{19}$$

where $f_{\rm EM}^{\rm fb} \sim 0.05$ is the fraction of electromagnetic energy emitted by the fireball. We arrived at $f_{\rm EM}^{\rm fb}$ from considering the π^0 fraction, equal to $1/3$ the total π fraction, as before. By substituting our fiducial numbers in (19) it is straightforward to see that the hadronic shower is increased by about 30% if $n'_{\rm gen} = 8$ and by about 70% if $n'_{\rm gen} = 7$, in agreement with recent Auger results [5].

Of course, (19) is a dreadful simplification of the shower evolution. As we have noted before, the shower evolution depends on primary energy, as well as the elasticity and particle multiplicity which also depend on E. Note that all these restrictions have not been specified explicitly as separate parameters in (19), but rather as a combined constant $n'_{\rm gen}$. Moreover, heavy meson production must also be taken into consideration when modeling the shower

[5]The average neutrino energy from the direct pion decay is $\langle E_\nu \rangle = (1 - r)E_\pi/2 \simeq 0.22E_\pi$ and that of the muon is $\langle E_\mu \rangle = (1 + r)E_\pi/2 \simeq 0.78E_\pi$, where $r = 0.573$ is the ratio of the muon to the pion mass squared. Thus, we can safely neglect the missing energy in neutrinos.

evolution (distinctively, η and η' contribute about 4% to the electromagnetic cascade). Unfortunately, it is difficult to estimate accurate parameter values of the shower evolution in a simple analytical fashion. For such a situation, a full-blown simulation may be the only practical approach.

As a second-order approximation, we estimate the fireball spectrum and propagate the particles in the atmosphere using the algorithms of AIRES (version 2.1.1) [50]. Most of the large multiplicity of observable quanta emitted in the fireball is expected to come through hadronic jets produced by the quarks. We assume that $A/2$ nucleons (each with initial energy E/A) produce the fireball and that the remaining nucleons scatter inelastically at the collision vertex. We further assume that for the nucleons producing the fireball, each of the valence quarks interact to give dijet final states without any leading particle. We calculate the total energy of each jet $E_{\rm jet}$ in the rest frame of the fireball from the momentum fraction carried by the up and down quarks, using CTEQ6L parton distribution functions [51].

The precise nature of the fragmentation process is unknown. We adopt the quark → hadron fragmentation spectrum originally suggested by Hill,

$$\frac{dN_h}{dx} \approx 0.08 \exp\left[2.6\sqrt{\ln(1/x)}\right](1-x)^2 \times \left[x\sqrt{\ln(1/x)}\right]^{-1}, \tag{20}$$

where $x \equiv E_h/E_{\rm jet}$, with E_h being the energy of any hadron in the jet. This is consistent with the so-called "leading-log QCD" behavior and seems to reproduce quite well the multiplicity growth seen in collider experiments [52]. $dN_h/dx \approx (15/16)x^{-3/2}(1-x)^2$ provides a reasonable parametrization of (20) for $10^{-3} < x < 1$. And so we set the infrared cutoff to $x_{\rm cut} = 10^{-3}$. The main features of the jet fragmentation process derived from this simplified parametrization are listed in Table I. Using the multiplicity ratios derived in the previous section and the fractional equivalent energies given in Table I, we construct the fireball particle spectra. More specifically, for each jet, we start first from $x = 1$ and integrate down in x until three leading hadron particles are obtained. The resulting interval in x is $\Delta x \equiv (x_2 = 1) - x_1$, as shown in column 3, with x_2 and x_1 values listed in columns 2 and 1, respectively. We assign one of three species types to each hadron using the $\pi:K:N$ weights. The energy fraction of the jet contained in these three hadrons is given in column 4, and the average energy fraction for each of these three hadrons, denoted $x_{\rm equivalent}$, is given in column 5. Next, we duplicate the procedure for the remaining hadron species following the splitting of fractional energies, $\int_{x_1}^{x_2} N_h dx$, as given in column 3, and assigning to each hadron in the interval the corresponding $x_{\rm equivalent}$ from column 5. Note that for each subsequent Δx interval, the fractional hadron energy $x_{\rm equivalent}$ is significantly smaller; this feature allows us to sensibly truncate the process after five intervals at our cutoff value $x_{\rm cut}$. The mean energy of each of the fifth and final batch of 30 hadrons produced by wee partons is $\sim 1/100$ of the energy of each hadron produced by large x partons in first batch. The average particle multiplicity per jet is the sum of the column 3 entries, approximately 54. Charge and strangeness conservation are separately imposed by hand.

TABLE I. Properties of jet hadronization [53]. Columns 1 and 2 define the interval $\Delta x = x_2 - x_1$ over which N_h hadrons are made. N_h is listed in the third column. Column 4 presents the fractional energy of the jet contained in these N_h hadrons, and column 5 gives the mean fractional energy for each of these hadrons ($x_{\rm equivalent}$).

x_1	x_2	$\int_{x_1}^{x_2} N_h dx$	$\int_{x_1}^{x_2} x N_h dx$	$x_{\rm equivalent}$
0.0750	1.0000	3	0.546	0.182
0.0350	0.0750	3	0.155	0.052
0.0100	0.0350	9	0.167	0.018
0.0047	0.0100	9	0.062	0.007
0.0010	0.0047	30	0.069	0.002

All secondary particles are boosted to the laboratory frame. The particles are tightly beamed due to their very high boost. The boosted secondaries are then injected into AIRES as primaries of an air shower initiated at the collision vertex. The vertex of the primary interaction is determined using the mean free path of a ^{14}N nucleus with $E = 10^{10}$ GeV. We set the observation point at 1.5 km above sea level, which is the altitude of Auger. All shower particles with energies above the following thresholds were tracked: 750 keV for gammas, 900 keV for electrons and positrons, 10 MeV for muons, 60 MeV for mesons, and 120 MeV for nucleons. The geomagnetic field was set to reproduce that prevailing upon the Auger experiment. For further details, see Appendix C. Secondary particles of different types in individual showers were sorted according to their distance d to the shower axis. Our results are encapsulated in Fig. 1, where we compare the density distribution of $\mu^{\pm}$ at ground level for a typical nitrogen shower processed by the AIRES kernel with that of a nitrogen fireball explosion. The vertical axis is given in arbitrary units to indicate the large systematic uncertainty in the normalization of the lateral distribution, which is induced by the different predictions of high-energy hadronic event generators. Importantly, the comparison of hadron and fireball fluxes is *not* arbitrary. It is easily seen that the number of muons at $d = 1$ km is about 40% higher in the fireball-induced shower.

The third-order approximation should include a precise determination of the fireball particle spectra using scaling hydrodynamic equations, which contain the probability amplitudes for $s\bar{s}$ production and annihilation both in the fireball phase and in the hadron gas phase [54–59]. It should also contain a thorough high-level competitive

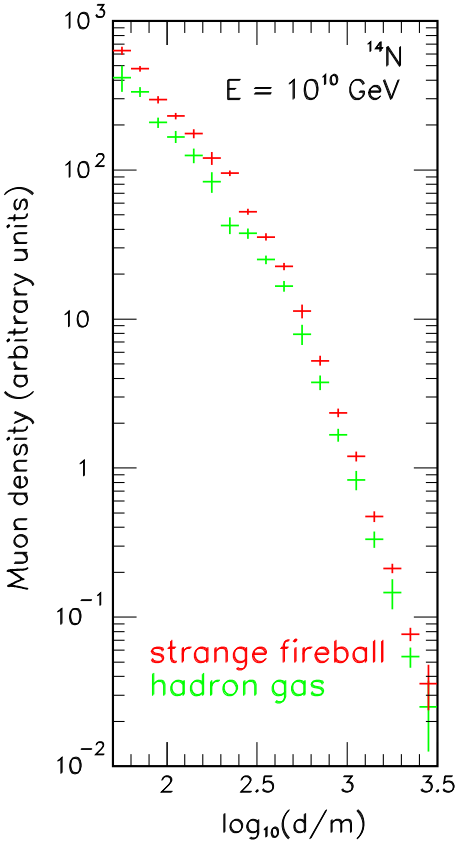

FIG. 1. Density distributions at ground level of $\mu^{\pm}$ as a function of the distance d to the shower axis. The error bars indicate the rms fluctuations.

analysis of theoretical systematics emanating from hadronic interaction models. This rather ambitious project is beyond the scope of this paper, but will be the topic of a future publication.

IV. CONCLUSIONS

Teasing out the physics of ultrahigh-energy cosmic rays has proven to be extraordinarily challenging. The Pierre Auger Observatory employs several detection methods to extract complementary information about the extensive air showers produced by ultrahigh-energy cosmic rays [12]. Two types of instruments are employed: Cherenkov particle detectors on the ground sample air-shower fronts as they arrive at Earth's surface, whereas fluorescence telescopes measure the light produced by air-shower particles exciting atmospheric nitrogen. These two detector systems provide complementary information, as the surface detector (SD) measures the lateral distribution and time structure of shower particles arriving at the ground, and the fluorescence detector (FD) measures the longitudinal development of the shower in the atmosphere. A subset of *hybrid* showers is observed simultaneously by the SD and FD. These are very precisely measured and provide an invaluable tool for energy calibration, minimizing systematic uncertainties and studying composition by simultaneously using SD and FD information. Very recently, the Pierre Auger Collaboration exploited the information in individual hybrid events initiated by cosmic rays with $10^{9.8} \lesssim E/\mathrm{GeV} \lesssim 10^{10.2}$ to study hadronic interactions at ultrahigh energies [5]. The analysis indicates that the observed hadronic signal of these showers is significantly larger (30% to 60%) than predicted by the leading LHC-tuned models, with a corresponding excess of muons. The significance of the discrepancy between the data (411 hybrid events) and the model prediction is above about 2.1σ. A deployment of a 4 m^2 scintillator on top of each SD is foreseen as a part of the AugerPrime upgrade of the Observatory to measure the muon and electromagnetic contributions to the ground signal separately [60]. This will provide additional information to reduce systematic uncertainties and perhaps increase the significance of the muon excess.

Even though the excess is not statistically significant yet, it is interesting to entertain the possibility that it corresponds to a real signal of QCD dynamics flagging the onset of deconfinement. In this paper, we have proposed a model that can explain the observed excess in the muon signal. We have assumed that ultrarelativistic nuclei ($E \gtrsim 10^{9.8}$ GeV) that collide in the upper atmosphere could create a deconfined thermal fireball which undergoes a sudden hadronization. At production, the fireball has a very high matter density and consists of gluons and two flavors of light quarks (u, d). Because the fireball is formed in the baryon-rich projectile fragmentation region, the high baryochemical potential damps the production of $u\bar{u}$ and $d\bar{d}$ pairs, resulting in gluon fragmentation mainly into $s\bar{s}$. The strange quarks then become much more abundant and upon hadronization the relative density of strange hadrons is significantly enhanced over that resulting from a hadron gas. We have shown that the augmented production of strange hadrons by the fireball, over that resulting from a hadron gas alone, provides a mechanism to increase the muon content in atmospheric cascades by about 40%, in agreement with the data of the Auger facility.

Contrary to previous proposals [13–15] to explain the muon excess in Auger data our model relies on the assumption that ultrahigh-energy cosmic rays are heavy (or medium mass) nuclei. As noted elsewhere [61], upper limits on the cosmic diffuse neutrino flux provide a constraint on the proton fraction in ultrahigh-energy cosmic rays, and therefore can be used to set indirect constraints on the model proposed herein. In particular, the nearly guaranteed flux of cosmogenic neutrinos is a decay product from the generated pions in interactions of ultrahigh-energy cosmic rays with the cosmic microwave background and related radiation [62]. The spectral shape and intensity of this flux depend on whether the cosmic-ray particles are protons or heavy nuclei. For proton primaries, the energy-squared-weighted flux peaks between $10^{9.6}$ and 10^{10} GeV,

and the intensity is around 1 in Waxman-Bahcall (WB) units [63–70].[6] For heavy nuclei, the peak is at much lower energy (around $10^{8.7}$ GeV [72,73]) and the intensity is about 0.1 to 0.01 WB, depending on source evolution [69,70]. The sensitivity of existing neutrino-detection facilities has a reach to 1 WB, challenging cosmic-ray models for which the highest energies are proton dominated [74–81]. Next-generation neutrino detectors will systematically probe the entire range of the parameter space of cosmogenic neutrinos [82–87]. Observation of the cosmogenic neutrino flux with an intensity of 0.1 to 0.01 WB could become the smoking gun for the ideas discussed in this paper. Complementary information can be obtained with accompanying cosmogenic photons [88]. As a matter of fact, the Pierre Auger Observatory has begun to probe the region of the parameter space relevant for proton primaries [89]. A third probe of proton-dominated ultrahigh-energy cosmic ray models is the extragalactic gamma-ray background seen by Fermi-LAT (and, in the future, CTA) [79,90]. For heavy nuclei, however, the cosmogenic photon intensity is almost negligible and therefore cannot be used (for the time being) as a harbinger signal [91].

For $10^{9.5} \lesssim E/\mathrm{GeV} \lesssim 10^{10.6}$, the mean and dispersion of $X_{\max}$ inferred from the fluorescence Auger data point to a light composition (protons and helium) towards the low end of this energy bin and to a large light-nuclei content (around helium) towards the high end (see Fig. 3 in [92]). However, when the signal in the water Cherenkov stations (with sensitivity to both the electromagnetic and muonic components) is correlated with the fluorescence data, a light composition made up of only proton and helium becomes inconsistent with observations [93]. The hybrid data indicate that intermediate nuclei, with $A \simeq 14$, must contribute to the energy spectrum in this energy bin. Moreover, a potential iron contribution cannot be discarded.

At this stage, it is worthwhile to point out that the production of a fireball may modify the shower evolution. For example, after emitting K^+ and K^0, the fireball has a finite excess of s quarks, and because of the s quarks' stabilizing effects, the fireball could form heavy multiquark droplets S, with large strangeness [94–98]. The energy lost by the S particles during collision with nucleons is primarily through hard scattering, and so the fractional energy loss per collision is $\sim \mathrm{GeV}/M_S$ [99,100]. S production may thus slow down the shower evolution. Although this effect has not been included in our simulations, one may wonder whether the structure observed in the elongation rate above about $10^{10.4}$ GeV [101] could be ascribed to the onset of S production. Of course one would not expect a fireball to be created when nuclei just slide along each other. The admixture of peripheral and fireball collisions would then produce large fluctuations in the number of muons at ground level. However, since the critical energy for charged pions $\xi_c^{\pi^\pm}$ and kaons $\xi_c^{K^\pm}$ is roughly the same, the elongation rate of the muon channel would be almost unaltered and so the muon shower maximum $X_{\mu,\max}$ would have small fluctuations. Moreover, if the fireball indeed modifies the elongation rate of the electromagnetic shower, the peripheral collisions would also tend to increase the dispersion of $X_{\max}$, mimicking what is expected for a light composition in the canonical framework where no fireballs are being produced in this energy range.

In closing, we comment on the differences between our model and the proposal by Farrar and Allen (FA) [13], which also relies on QCD dynamics at high temperature. To better understand the differences between these models we first note that at low energies, QCD exhibits two interesting phenomena: confinement and (approximate) spontaneous chiral symmetry breaking. These two phenomena are strong-coupling effects, invisible to perturbation theory. The confinement force couples quarks to form hadrons and the chiral force binds the collective excitations to Goldstone bosons.

As a matter of course, there is no relation *a priori* between these two phenomena; in thermodynamics, the associated scales are characterized by two distinct temperatures, T_c and T_χ. For $T > T_c$, hadrons dissolve into quarks and gluons, whereas for $T > T_\chi$, the chiral symmetry is fully restored and quarks become massless, forming an ideal quark-gluon plasma. The $\mu_B - T$ phase diagram of hadronic matter thus contains a *confined phase* consisting of an interacting gas of hadrons (a *resonance gas*) and a *deconfined phase* comprising a (nonideal) gas of quarks and gluons [102]. The *phase boundary* reflects the present uncertainties from lattice QCD extrapolated to finite baryochemical potential. The intermediate region in between the hadron gas and the ideal quark-gluon plasma is the domain of the thermal fireball. The existence of this intermediate region with deconfined massive quarks and gluons is also conjectured from high-statistics lattice-QCD calculations, which indicate that, for $T \sim 3T_c$, the energy density is about 85% of the Stefan-Boltzmann energy density for the ideal quark-gluon plasma [27]. Note that this temperature is not inconsistent with our estimate in (16). In the FA model, the pion suppression is a direct consequence of massless quarks living above the chiral symmetry restoration temperature, i.e., $T > T_\chi$. In our model, however, the pion suppression is the result of the large baryochemical potential which forbids the creation of light $u\bar{u}$ and $d\bar{d}$ pairs, allowing abundant production of massive $s\bar{s}$ via gluon fragmentation. This process naturally occurs in the fireball boundary phase (where $T < T_\chi$), and is a consequence of the high nucleon density of Lorentz-boosted nuclei. In principle, it is possible that the muon excess observed in Auger data originates in a combination of these two high-temperature QCD phenomena. Note that if ultrahigh-energy cosmic rays are heavy (or medium

[6] $1\ \mathrm{WB} = \mathrm{GeV}(\mathrm{cm}^2\,\mathrm{s}\,\mathrm{sr})^{-1}$ [71].

mass) nuclei and the observed muon excess is not the result of a large baryochemical potential suppressing the production of $u\bar{u}$ and $d\bar{d}$ pairs, but rather an effect of chiral symmetry restoration, then the excess should also be visible at $\sqrt{s} \approx 80$ TeV, which corresponds to the center-of-mass energy in collisions of projectile cosmic-ray protons with $E \approx 10^{9.5}$ GeV. This disparity could be used to discriminate among dominance between these two pion-suppression mechanisms.

On the one hand, a model consistent with all data requiring heavy nuclei at the high-energy end of the spectrum is generally considered a bit disappointing [103], especially for neutrino and cosmic-ray astronomy. On the other hand, we have shown that even if heavy nuclei dominate at the highest energies, upon scattering in Earth's atmosphere these nuclei could become compelling probes of QCD dynamics at high temperatures, particularly in the not-so-well-understood fireball boundary phase. Should this be the case, future AugerPrime data would provide relevant information on the strange quark density of the nucleon, complementing measurements at heavy-ion colliders.

ACKNOWLEDGMENTS

We would like to acknowledge many useful discussions with our colleagues of the Pierre Auger Collaboration. L. A. A. is supported by U.S. National Science Foundation (NSF) Grant No. PHY-1620661 and by National Aeronautics and Space Administration (NASA) Grant No. NNX13AH52G. T. J. W. is supported in part by Department of Energy (DOE) Grant No. DE-SC0011981.

APPENDIX A: FERMI-DIRAC AND BOSE-EINSTEIN INTEGRALS

For the sake of completeness, in this appendix we provide all of the formulas used for computing the number densities of $\bar{s}$, $\bar{q}$, and g.

The Fermi-Dirac and Bose-Einstein distributions (6) can be rewritten as infinite sums of Boltzmann distributions,

$$f(p)_{i,\pm} = \frac{1}{(2\pi)^3}\frac{1}{e^{(\sqrt{p^2+m_i^2}-\mu_i)/T} \pm 1} = \frac{1}{(2\pi)^3}\sum_{n=1}^{\infty}(\mp)^{n+1}e^{-n(\sqrt{p^2+m_i^2}-\mu_i)/T}. \quad \text{(A1)}$$

Following [104] we introduce the dimensionless variables, z and τ:

$$z = \frac{m_i}{T}; \qquad \tau = \frac{\sqrt{p^2+m_i^2}}{T}; \qquad |p| = T\sqrt{\tau^2 \div z^2}$$
$$|p|d|p| = T^2\tau d\tau; \qquad |p|^2 d|p| = T^3\tau\sqrt{\tau^2 - z^2}\,d\tau.$$

In terms of τ and z, the number density for the Boltzmann distribution can be written as

$$n_i^{\mathrm{B}} = \int \frac{d^3p}{(2\pi)^3}e^{(\mu_i-\sqrt{p^2+m_i^2})/T} = 4\pi\frac{T^3}{(2\pi)^3}e^{\mu_i/T}\int_z^{\infty} d\tau(\tau^2-z^2)^{1/2}\tau e^{-\tau}. \quad \text{(A2)}$$

A closed form expression can be found for n_i^{B} in terms of the modified Bessel function

$$K_n(z) = \frac{2^n n!}{(2n)!}\frac{1}{z^n}\int_z^{\infty} d\tau(\tau^2-z^2)^{n-1/2}e^{-\tau}. \quad \text{(A3)}$$

Note that $K_n(z)$ has another representation, which follows from (A3) by partial integration,

$$K_n(z) = \frac{2^{n-1}(n-1)!}{(2n-2)!}\frac{1}{z^n}\int_z^{\infty}\tau(\tau^2-z^2)^{n-3/2}\tau e^{-\tau}. \quad \text{(A4)}$$

The modified Bessel function has a recurrence relation,

$$K_{n+1}(z) = \frac{2nK_n(z)}{z} + K_{n-1}(z), \quad \text{(A5)}$$

such that if the expressions for $K_0(z)$ and $K_1(z)$ are known, all the others can be easily obtained. From (A4) it is straightforward to obtain

$$K_2(z) = \frac{1}{z^2}\int_z^{\infty}\tau(\tau^2-z^2)^{1/2}\tau e^{-\tau}, \quad \text{(A6)}$$

and so (A2) becomes

$$n_i^{\mathrm{B}} = \frac{T^3}{2\pi^2}z^2K_2(z) = \frac{T^3}{2\pi^2}\left(\frac{m_i}{T}\right)^2 K_2\left(\frac{m_i}{T}\right)e^{\mu_i/T}. \quad \text{(A7)}$$

For the Fermi-Dirac distribution, the number density is found to be

$$n_i^{\mathrm{FD}} = \frac{T^3}{2\pi^2}\sum_{n=1}^{\infty}(-1)^{n+1}\frac{1}{n^3}\left(\frac{nm_i}{T}\right)^2 K_2\left(\frac{nm_i}{T}\right)e^{n\mu_i/T}. \quad \text{(A8)}$$

For the Bose-Einstein distribution, the number density is given by

$$n_i^{\mathrm{BE}} = \frac{T^3}{2\pi^2}\sum_{n=1}^{\infty}\frac{1}{n^3}\left(\frac{nm_i}{T}\right)^2 K_2\left(\frac{nm_i}{T}\right)e^{n\mu_i/T}. \quad \text{(A9)}$$

In the limit $m_i \to 0$ and $\mu_i \to 0$ we immediately obtain

$$n_i^{\mathrm{BE}} = \frac{T^3}{\pi^2}\sum_{n=1}^{\infty}\frac{1}{n^3} = \frac{T^3}{\pi^2}\zeta(3), \quad \text{(A10)}$$

where $\zeta(x)$ is the Riemann function. Finally, using (A8) and (A10), it is straightforward to obtain (8), (9), and (11).

APPENDIX B: $\mu_B \leftrightharpoons T$ CONNECTION

Our best understanding of the thermodynamical properties of QCD at vanishing baryon density is rooted on high-statistics lattice-QCD numerical simulations. However, if the baryon density is nonzero, these simulations break down. The only physically relevant analyses for which the obstacles of lattice QCD can be circumvented are those dealing with small baryon density or, more accurately, small μ_B. Namely, if we are interested in the observable $O(\mu_B)$, we can expand it in powers of μ_B as

$$O(\mu_B) = O_0 + O_1\mu_B + O_2\mu_B^2 + \cdots \tag{B1}$$

and try to determine the series coefficients [105]. Which values of μ_B can be considered *small enough* to give reliable results with this procedure is something that can only be determined *a posteriori* by the convergence property of the series, limited by the accuracy in the evaluation of the expansion coefficients. One such observable is the quark-hadron crossover line. Data from heavy-ion colliders suggest that the energy dependence of this line can be parametrized as

$$T(\mu_B) = a - b\mu_B^2 - c\mu_B^4, \tag{B2}$$

with $a = (0.166 \pm 0.002)\,\mathrm{GeV}$, $b = (0.139 \pm 0.016)\,\mathrm{GeV}^{-1}$, and $c = (0.053 \pm 0.021)\,\mathrm{GeV}^{-3}$, and that the baryochemical potential can be parametrized as

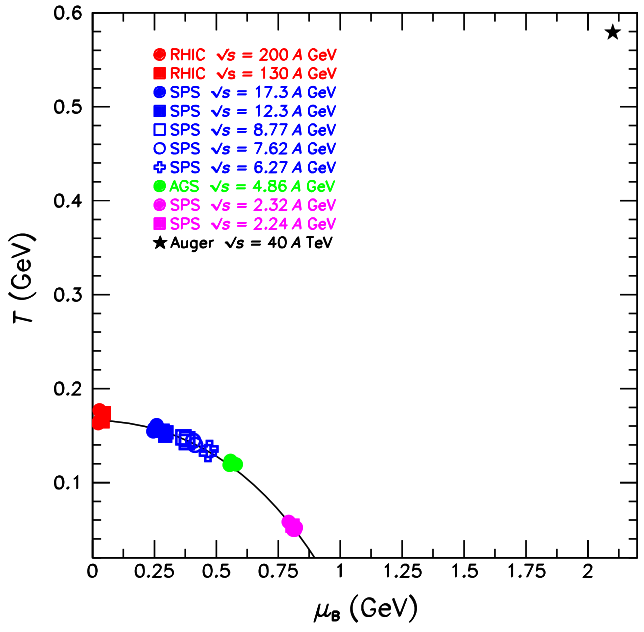

FIG. 2. Relation between μ_B and T as obtained in statistical-thermal model fits to Au + Au and Pb + Pb collision systems by numerous groups [116–127] over a wide range of energies. The solid line is the parametrization (B2). The lower left-hand corner is dominantly the hadron phase. The region above the crossover line is dominantly the quark-gluon fireball phase. The black star indicates the required value for our model to describe Auger data.

$$\mu_B(\sqrt{s}) = \frac{a}{1 + b\sqrt{s}}, \tag{B3}$$

with $a = (1.308 \pm 0.028)$ GeV and $b = (0.273 \pm 0.008)\ \mathrm{GeV}^{-1}$ [106]. Interestingly, the lattice-QCD calculation converges towards the quark-hadron crossover line as $\mu_B \to 0$ [107,108], but it appears to depart from this line at large values of μ_B [109]. This a widely discussed feature [110–114] which has, however, not been conclusively understood. (Several hadronization schemes have been proposed, see e.g. [115]. They differ in the geometry and in the flow velocity profile.) This perplexing region may well be relevant to cosmic-ray observations. Our results in the region shown in Fig. 2 suggest that this is so.

APPENDIX C: MONTE CARLO SIMULATION OF AIR SHOWERS

The AIRES simulation engine [50] provides full space-time particle propagation in a realistic environment, taking into account the characteristics of the atmospheric density profile (using the standard U.S. atmosphere), Earth's curvature, and the geomagnetic field (calculated for the location of Auger with an uncertainty of a few percent [128]). The following particles are tracked in the Monte Carlo simulation: photons, electrons, positrons, muons, pions, kaons, eta mesons, lambda baryons, nucleons, antinucleons, and nuclei up to $Z = 36$. The high-energy collisions are processed by invoking external hadronic event generators, whereas the low-energy ones are processed using an extension of the Hillas splitting algorithm [129].

The AIRES program consists of various interacting procedures that operate on a data set with a variable number of records. Several data arrays (or stacks) are defined. Every record within each of these stacks is a particle entry and represents a physical particle. The data contained in every record are related to the characteristics of the corresponding particle. The particles can move inside a volume within the atmosphere where the shower takes place. This volume is limited by the ground, the injection surfaces, and by vertical planes which limit the region of interest. Before starting the simulation, all the stacks are empty. The first action is to add the first stack entry, which corresponds to the primary particle. Then the stack processing loop begins. The primary is initially located at the injection surface, and its downwards direction of motion defines the shower axis. After the primary's fate has been decided, the corresponding interaction begins to be processed. The latter generally involves the creation of new particles which are stored in the empty stacks and remain waiting to be processed. Particle entries are removed when one of the following events happen: (i) the energy of the particle is below the selected cut energy; (ii) the particle reaches ground level; (iii) a particle going upwards reaches

the injection surface; and (iv) a particle with quasihorizontal motion exists in the region of interest. After having scanned all the stacks, it is checked whether or not there are new particle entries pending further processing. If the answer is positive, then all the stacks are scanned once more; otherwise the simulation of the shower is complete.

For the present analysis, we use the AIRES module for *special* and/or *multiple primary particles*. This useful feature allows us to dynamically call a user-defined module that tracks the interactions of a bundle of particles returning a handy list of secondaries, which can be conveniently controlled by the propagating engine for further processing.

[1] L. A. Anchordoqui, M. T. Dova, L. N. Epele, and S. J. Sciutto, Hadronic interactions models beyond collider energies, Phys. Rev. D **59**, 094003 (1999).

[2] C. A. G. Canal, S. J. Sciutto, and T. Tarutina, Testing hadronic interaction packages at cosmic ray energies, Phys. Rev. D **79**, 054006 (2009).

[3] P. Gondolo, G. Ingelman, and M. Thunman, Charm production and high-energy atmospheric muon and neutrino fluxes, Astropart. Phys. **5**, 309 (1996).

[4] C. Patrignani *et al.* (Particle Data Group Collaboration), Review of particle physics, Chin. Phys. C **40**, 100001 (2016).

[5] A. Aab *et al.* (Pierre Auger Collaboration), Testing Hadronic Interactions at Ultrahigh Energies with Air Showers Measured by the Pierre Auger Observatory, Phys. Rev. Lett. **117**, 192001 (2016).

[6] L. Anchordoqui, M. T. Dova, A. G. Mariazzi, T. McCauley, T. C. Paul, S. Reucroft, and J. Swain, High energy physics in the atmosphere: Phenomenology of cosmic ray air showers, Ann. Phys. (Amsterdam) **314**, 145 (2004).

[7] D. d'Enterria, R. Engel, T. Pierog, S. Ostapchenko, and K. Werner, Constraints from the first LHC data on hadronic event generators for ultra-high energy cosmic-ray physics, Astropart. Phys. **35**, 98 (2011).

[8] R. Ulrich, R. Engel, and M. Unger, Hadronic multiparticle production at ultrahigh energies and extensive air showers, Phys. Rev. D **83**, 054026 (2011).

[9] T. Abu-Zayyad *et al.* (HiRes and MIA Collaborations), Evidence for Changing of Cosmic Ray Composition between 10^{17} eV and 10^{18} eV from Multicomponent Measurements, Phys. Rev. Lett. **84**, 4276 (2000).

[10] A. Aab *et al.* (Pierre Auger Collaboration), Muons in air showers at the Pierre Auger Observatory: Mean number in highly inclined events, Phys. Rev. D **91**, 032003 (2015); Erratum, Phys. Rev. D **91**, 059901(E) (2015).

[11] Yu. A. Fomin, N. N. Kalmykov, I. S. Karpikov, G. V. Kulikov, M. Yu. Kuznetsov, G. I. Rubtsov, V. P. Sulakov, and S. V. Troitsky, No muon excess in extensive air showers at 100–500 PeV primary energy: EAS-MSU results, arXiv:1609.05764.

[12] A. Aab *et al.* (Pierre Auger Collaboration), The Pierre Auger cosmic ray observatory, Nucl. Instrum. Methods Phys. Res., Sect. A **798**, 172 (2015).

[13] G. R. Farrar and J. D. Allen, A new physical phenomenon in ultrahigh energy collisions, Eur. Phys. J. Web Conf. **53**, 07007 (2013).

[14] J. Allen and G. Farrar, in *Proceedings of the 33rd International Cosmic Ray Conference (ICRC2013), Rio de Janeiro, 2013*, edited by A. Saa and R. C. Shellard (to be published).

[15] J. Alvarez-Muñiz, L. Cazon, R. Conceição, J. Dias de Deus, C. Pajares, and M. Pimenta, Muon production and string percolation effects in cosmic rays at the highest energies, arXiv:1209.6474.

[16] F. Halzen and H. C. Liu, Evidence for stabilized strange quark matter in cosmic rays?, Phys. Rev. D **32**, 1716 (1985).

[17] A. D. Panagiotou, A. Karabarbounis, and A. Petridis, Abnormal photonic energy: A signal of quark matter possibly seen in exotic cosmic ray events, Z. Phys. A **333**, 355 (1989).

[18] A. D. Panagiotou, A. Petrides, and M. Vassiliou, Possibility of observing "Centauro", events at the BNL Relativisic Heavy Ion Collider, Phys. Rev. D **45**, 3134 (1992).

[19] M. N. Asprouli, A. D. Panagiotou, and E. Gladysz-Dziadus, Interaction length and spontaneous decay of a cosmic ray "Centauro", fireball, Astropart. Phys. **2**, 167 (1994).

[20] A. L. S. Angelis, E. Gladysz-Dziadus, Y. V. Kharlov, V. L. Korotkikh, G. Mavromanolakis, A. D. Panagiotou, and S. A. Sadovsky, Model of Centauro and strangelet production in heavy ion collisions, Yad. Fiz. **67**, 414 (2004) [Phys. At. Nucl. **67**, 396 (2004)].

[21] J. C. Collins and M. J. Perry, Superdense Matter: Neutrons or Asymptotically Free Quarks?, Phys. Rev. Lett. **34**, 1353 (1975).

[22] F. Iachello, W. D. Langer, and A. Lande, A quark-like model of high-density matter, Nucl. Phys. **A219**, 612 (1974).

[23] N. Cabibbo and G. Parisi, Exponential hadronic spectrum and quark liberation, Phys. Lett. **59B**, 67 (1975).

[24] D. J. Gross and F. Wilczek, Ultraviolet Behavior of Non-Abelian Gauge Theories, Phys. Rev. Lett. **30**, 1343 (1973).

[25] H. D. Politzer, Reliable Perturbative Results for Strong Interactions?, Phys. Rev. Lett. **30**, 1346 (1973).

[26] J. D. Bjorken, Highly relativistic nucleus-nucleus collisions: The central rapidity region, Phys. Rev. D **27**, 140 (1983).

[27] A. Bazavov *et al.*, Equation of state and QCD transition at finite temperature, Phys. Rev. D **80**, 014504 (2009).

[28] D. Ivanenko and D. F. Kurdgelaidze, Remarks on quark stars, Lett. Nuovo Cimento **2**, 13 (1969).

[29] N. Itoh, Hydrostatic equilibrium of hypothetical quark stars, Prog. Theor. Phys. **44**, 291 (1970).
[30] G. Chapline, Jr. and M. Nauenberg, Phase transition from baryon to quark matter, Nature (London) **264**, 235 (1976).
[31] B. Freedman and L. D. McLerran, Quark star phenomenology, Phys. Rev. D **17**, 1109 (1978).
[32] G. Chapline and M. Nauenberg, On the possible existence of quark stars, Ann. N.Y. Acad. Sci. **302**, 191 (1977).
[33] C. Alcock, E. Farhi, and A. Olinto, Strange stars, Astrophys. J. **310**, 261 (1986).
[34] A. V. Olinto, On the conversion of neutron stars into strange stars, Phys. Lett. B **192**, 71 (1987).
[35] R. Anishetty, P. Koehler, and L. D. McLerran, Central collisions between heavy nuclei at extremely high-energies: The fragmentation region, Phys. Rev. D **22**, 2793 (1980).
[36] F. Halzen and H. C. Liu, Comprehensive Explanation of Cosmic Ray "Anomalies": Quark Matter Formation by Heavy Nuclear Primaries, Phys. Rev. Lett. **48**, 771 (1982).
[37] J. Cleymans, M. Dechantsreiter, and F. Halzen, Formation and signature of quark matter in relativistic ion collisions: Evidence from cosmic rays, Z. Phys. C **17**, 341 (1983).
[38] F. Halzen, The search for matter in its quark-gluon phase, Contemp. Phys. **24**, 591 (1983).
[39] V. Khachatryan *et al.* (CMS Collaboration), Transverse-Momentum and Pseudorapidity Distributions of Charged Hadrons in pp Collisions at $\sqrt{s} = 7$ TeV, Phys. Rev. Lett. **105**, 022002 (2010).
[40] D. d'Enterria, R. Engel, T. Pierog, S. Ostapchenko, and K. Werner, The strong interaction at the collider and cosmic-rays frontiers, Few-Body Syst. **53**, 173 (2012).
[41] J. Rafelski, Strangeness production in the quark gluon plasma, Nucl. Phys. **A418**, 215C (1984).
[42] N. K. Glendenning and J. Rafelski, Kaons and quark gluon plasma, Phys. Rev. C **31**, 823 (1985).
[43] E. W. Kolb and M. S. Turner, The early Universe, Front. Phys. **69**, 1 (1990).
[44] B. Muller, Physics and signatures of the quark-gluon plasma, Rep. Prog. Phys. **58**, 611 (1995).
[45] M. N. Asprouli and A. D. Panagiotou, Strangeness as probe of quark-gluon plasma: Unconventional point of view, Phys. Rev. C **51**, 1444 (1995).
[46] E. Gladysz-Dziadus, Are Centauros exotic signals of the QGP?, Pis'ma Fiz. Elem. Chast. At. Yadra **34**, 565 (2003) [Phys. Part. Nucl. **34**, 285 (2003)].
[47] O. Kaczmarek and F. Zantow, Static quark anti-quark interactions in zero and finite temperature QCD I: Heavy quark free energies, running coupling and quarkonium binding, Phys. Rev. D **71**, 114510 (2005).
[48] J. Rafelski, J. Letessier, and A. Tounsi, Strange particles from dense hadronic matter, Acta Phys. Pol. B **27**, 1037 (1996).
[49] J. Matthews, A Heitler model of extensive air showers, Astropart. Phys. **22**, 387 (2005).
[50] S. J. Sciutto, AIRES: A system for air shower simulations, arXiv:astro-ph/9911331.
[51] J. Pumplin, D. R. Stump, J. Huston, H. L. Lai, P. M. Nadolsky, and W. K. Tung, New generation of parton distributions with uncertainties from global QCD analysis, J. High Energy Phys. 07 (2002) 012.
[52] C. T. Hill, Monopolonium, Nucl. Phys. **B224**, 469 (1983).
[53] L. Anchordoqui and H. Goldberg, Experimental signature for black hole production in neutrino air showers, Phys. Rev. D **65**, 047502 (2002).
[54] J. Rafelski and B. Muller, Strangeness Production in the Quark-Gluon Plasma, Phys. Rev. Lett. **48**, 1066 (1982); Erratum, Phys. Rev. Lett. **56**, 2334(E) (1986).
[55] J. Rafelski, Formation and observables of the quark-gluon plasma, *Phys. Rep.* 88, 331 (1982).
[56] J. I. Kapusta and A. Mekjian, How much strangeness production is there in ultrarelativistic nucleus nucleus collisions?, Phys. Rev. D **33**, 1304 (1986).
[57] T. Matsui, B. Svetitsky, and L. D. McLerran, Strangeness production in ultrarelativistic heavy-ion collisions. I. Chemical kinetics in the quark-gluon plasma, Phys. Rev. D **34**, 783 (1986); Erratum, Phys. Rev. D **37**, 844(E) (1988).
[58] T. Matsui, B. Svetitsky, and L. D. McLerran, Strangeness production in ultrarelativistic heavy-ion collisions. II. Evolution of flavor composition in scaling hydrodynamics, Phys. Rev. D **34**, 2047 (1986).
[59] P. Koch, B. Muller, and J. Rafelski, Strangeness in relativistic heavy ion collisions, Phys. Rep. **142**, 167 (1986).
[60] A. Aab *et al.* (Pierre Auger Collaboration), The Pierre Auger Observatory upgrade: Preliminary design report, arXiv:1604.03637.
[61] M. Ahlers, L. A. Anchordoqui, and S. Sarkar, Neutrino diagnostics of ultrahigh energy cosmic ray protons, Phys. Rev. D **79**, 083009 (2009).
[62] V. S. Berezinsky and G. T. Zatsepin, Cosmic rays at ultrahigh-energies (neutrino?), Phys. Lett. **28B**, 423 (1969).
[63] F. W. Stecker, Diffuse fluxes of cosmic high-energy neutrinos, Astrophys. J. **228**, 919 (1979).
[64] C. T. Hill and D. N. Schramm, Ultrahigh energy cosmic ray neutrinos, Phys. Lett. **131B**, 247 (1983).
[65] R. Engel, D. Seckel, and T. Stanev, Neutrinos from propagation of ultrahigh-energy protons, Phys. Rev. D **64**, 093010 (2001).
[66] Z. Fodor, S. D. Katz, A. Ringwald, and H. Tu, Bounds on the cosmogenic neutrino flux, J. Cosmol. Astropart. Phys. 11 (2003) 015.
[67] L. A. Anchordoqui, H. Goldberg, D. Hooper, S. Sarkar, and A. M. Taylor, Predictions for the cosmogenic neutrino flux in light of new data from the Pierre Auger Observatory, Phys. Rev. D **76**, 123008 (2007).
[68] M. Ahlers, L. A. Anchordoqui, M. C. Gonzalez-Garcia, F. Halzen, and S. Sarkar, GZK neutrinos after the Fermi-LAT diffuse photon flux measurement, Astropart. Phys. **34**, 106 (2010).
[69] K. Kotera, D. Allard, and A. V. Olinto, Cosmogenic neutrinos: Parameter space and detectabilty from PeV to ZeV, J. Cosmol. Astropart. Phys. 10 (2010) 013.
[70] K. H. Kampert and M. Unger, Measurements of the cosmic ray composition with air shower experiments, Astropart. Phys. **35**, 660 (2012).
[71] E. Waxman and J. N. Bahcall, High-energy neutrinos from astrophysical sources: An upper bound, Phys. Rev. D **59**, 023002 (1998).

[72] D. Hooper, A. Taylor, and S. Sarkar, The impact of heavy nuclei on the cosmogenic neutrino flux, Astropart. Phys. **23**, 11 (2005).
[73] M. Ave, N. Busca, A. V. Olinto, A. A. Watson, and T. Yamamoto, Cosmogenic neutrinos from ultrahigh energy nuclei, Astropart. Phys. **23**, 19 (2005).
[74] M. Ahlers and F. Halzen, Minimal cosmogenic neutrinos, Phys. Rev. D **86**, 083010 (2012).
[75] A. Aab *et al.* (Pierre Auger Collaboration), Improved limit to the diffuse flux of ultrahigh energy neutrinos from the Pierre Auger Observatory, Phys. Rev. D **91**, 092008 (2015).
[76] M. Unger, G. R. Farrar, and L. A. Anchordoqui, Origin of the ankle in the ultrahigh energy cosmic ray spectrum, and of the extragalactic protons below it, Phys. Rev. D **92**, 123001 (2015).
[77] R. Aloisio, D. Boncioli, A. di Matteo, A. F. Grillo, S. Petrera, and F. Salamida, Cosmogenic neutrinos and ultra-high energy cosmic ray models, J. Cosmol. Astropart. Phys. 10 (2015) 006.
[78] J. Heinze, D. Boncioli, M. Bustamante, and W. Winter, Cosmogenic neutrinos challenge the cosmic ray proton dip model, Astrophys. J. **825**, 122 (2016).
[79] A. D. Supanitsky, Implications of gamma-ray observations on proton models of ultrahigh energy cosmic rays, Phys. Rev. D **94**, 063002 (2016).
[80] M. G. Aartsen *et al.* (IceCube Collaboration), Constraints on Ultrahigh-Energy Cosmic-Ray Sources from a Search for Neutrinos above 10 PeV with IceCube, Phys. Rev. Lett. **117**, 241101 (2016).
[81] S. Yoshida, What have we learned about the sources of ultrahigh-energy cosmic rays via neutrino astronomy?, arXiv:1612.04934.
[82] P. Allison *et al.*, Design and initial performance of the Askaryan Radio Array prototype EeV neutrino detector at the South Pole, Astropart. Phys. **35**, 457 (2012).
[83] M. G. Aartsen *et al.* (IceCube Collaboration), IceCube-Gen2: A vision for the future of neutrino astronomy in Antarctica, arXiv:1412.5106.
[84] O. Martineau-Huynh *et al.* (GRAND Collaboration), The giant radio array for neutrino detection, Eur. Phys. J. Web Conf. **116**, 03005 (2016).
[85] S. Adrian-Martinez *et al.* (KM3Net Collaboration), Letter of intent for KM3NeT 2.0, J. Phys. G **43**, 084001 (2016).
[86] A. Neronov, D. V. Semikoz, L. A. Anchordoqui, J. Adams, and A. V. Olinto, Sensitivity of the space-based Cherenkov from astrophysical-neutrino telescope, Phys. Rev. D **95**, 023004 (2017).
[87] A. L. Connolly and A. G. Vieregg, Radio detection of high energy neutrinos, arXiv:1607.08232.
[88] D. Hooper, A. M. Taylor, and S. Sarkar, Cosmogenic photons as a test of ultra-high energy cosmic ray composition, Astropart. Phys. **34**, 340 (2011).
[89] A. Aab *et al.* (Pierre Auger Collaboration), Search for photons with energies above 10^{18} eV using the hybrid detector of the Pierre Auger Observatory, arXiv:1612.01517.
[90] V. Berezinsky, A. Gazizov, and O. Kalashev, Cascade photons as test of protons in UHECR, Astropart. Phys. **84**, 52 (2016).
[91] L. A. Anchordoqui, J. F. Beacom, H. Goldberg, S. Palomares-Ruiz, and T. J. Weiler, TeV γ Rays from Photodisintegration and Daughter Deexcitation of Cosmic-Ray Nuclei, Phys. Rev. Lett. **98**, 121101 (2007).
[92] A. Aab *et al.* (Pierre Auger Collaboration), Combined fit of spectrum and composition data as measured by the Pierre Auger Observatory, arXiv:1612.07155.
[93] A. Aab *et al.* (Pierre Auger Collaboration), Evidence for a mixed mass composition at the "ankle" in the cosmic-ray spectrum, Phys. Lett. B **762**, 288 (2016).
[94] E. Witten, Cosmic separation of phases, Phys. Rev. D **30**, 272 (1984).
[95] H. C. Liu and G. L. Shaw, Production and detection of metastable strange quark droplets in heavy ion collisions, Phys. Rev. D **30**, 1137 (1984).
[96] E. Farhi and R. L. Jaffe, Strange matter, Phys. Rev. D **30**, 2379 (1984).
[97] F. Halzen, in *Proceedings of the Workshop on Cosmic Ray and High-Energy Gamma Ray Experiments for the Space Station Era, Baton Rouge, 1984*, edited by W. V. Jones and J. P. Wefel (Louisiana State University, Baton Rouge, 1984).
[98] C. Greiner, P. Koch, and H. Stoecker, Separation of Strangeness from Antistrangeness in the Phase Transition from Quark to Hadron Matter: Possible Formation of Strange Quark Matter in Heavy-Ion Collisions, Phys. Rev. Lett. **58**, 1825 (1987).
[99] L. Anchordoqui, H. Goldberg, and C. Nunez, Probing split supersymmetry with cosmic rays, Phys. Rev. D **71**, 065014 (2005).
[100] L. A. Anchordoqui, A. Delgado, C. A. G. Canal, and S. J. Sciutto, Hunting long-lived gluinos at the Pierre Auger Observatory, Phys. Rev. D **77**, 023009 (2008).
[101] A. Aab *et al.* (Pierre Auger Collaboration), Depth of maximum of air-shower profiles at the Pierre Auger Observatory. I. Measurements at energies above $10^{17.8}$ eV, Phys. Rev. D **90**, 122005 (2014).
[102] R. Rapp and J. Wambach, Chiral symmetry restoration and dileptons in relativistic heavy ion collisions, Adv. Nucl. Phys. **25**, 1 (2000).
[103] R. Aloisio, V. Berezinsky, and A. Gazizov, Ultrahigh energy cosmic rays: The disappointing model, Astropart. Phys. **34**, 620 (2011).
[104] A. K. Chaudhuri, A short course on relativistic heavy ion collisions, arXiv:1207.7028.
[105] C. Bonati, M. D'Elia, M. Mariti, M. Mesiti, F. Negro, and F. Sanfilippo, Across the deconfinement, arXiv:1610.03338.
[106] J. Cleymans, H. Oeschler, K. Redlich, and S. Wheaton, Comparison of chemical freeze-out criteria in heavy-ion collisions, Phys. Rev. C **73**, 034905 (2006).
[107] F. Becattini, M. Bleicher, T. Kollegger, T. Schuster, J. Steinheimer, and R. Stock, Hadron Formation in Relativistic Nuclear Collisions and the QCD Phase Diagram, Phys. Rev. Lett. **111**, 082302 (2013).
[108] F. Becattini, J. Steinheimer, R. Stock, and M. Bleicher, Hadronization conditions in relativistic nuclear collisions and the QCD pseudo-critical line, Phys. Lett. B **764**, 241 (2017).

[109] A. Tawfik, QCD phase diagram: A Comparison of lattice and hadron resonance gas model calculations, Phys. Rev. D **71**, 054502 (2005).

[110] J. Letessier and J. Rafelski, Hadron production and phase changes in relativistic heavy ion collisions, Eur. Phys. J. A **35**, 221 (2008).

[111] L. McLerran, Strongly interacting matter at high energy density, Int. J. Mod. Phys. A **25**, 5847 (2010).

[112] A. Andronic *et al.*, Hadron production in ultra-relativistic nuclear collisions: Quarkyonic matter and a triple point in the phase diagram of QCD, Nucl. Phys. **A837**, 65 (2010).

[113] M. Li and J. I. Kapusta, High baryon densities in heavy ion collisions at energies attainable at the BNL Relativistic Heavy-Ion Collider and the CERN Large Hadron Collider, Phys. Rev. C **95**, 011901(R) (2017).

[114] L. McLerran, From the glasma to the QCD phase boundary, arXiv:1612.00864.

[115] G. Torrieri and J. Rafelski, Statistical hadronization probed by resonances, Phys. Rev. C **68**, 034912 (2003).

[116] J. Cleymans, B. Kampfer, M. Kaneta, S. Wheaton, and N. Xu, Centrality dependence of thermal parameters deduced from hadron multiplicities in $\mathrm{Au}+\mathrm{Au}$ collisions at $s(NN)^{(1/2)} = 130$ GeV, Phys. Rev. C **71**, 054901 (2005).

[117] P. Braun-Munzinger, D. Magestro, K. Redlich, and J. Stachel, Hadron production in Au-Au collisions at RHIC, Phys. Lett. B **518**, 41 (2001).

[118] F. Becattini, M. Gazdzicki, A. Keranen, J. Manninen, and R. Stock, Chemical equilibrium in nucleus nucleus collisions at relativistic energies, Phys. Rev. C **69**, 024905 (2004).

[119] F. Becattini, J. Manninen, and M. Gazdzicki, Energy and system size dependence of chemical freeze-out in relativistic nuclear collisions, Phys. Rev. C **73**, 044905 (2006).

[120] J. Cleymans, H. Oeschler, and K. Redlich, Influence of impact parameter on thermal description of relativistic heavy ion collisions at (1–2) A GeV, Phys. Rev. C **59**, 1663 (1999).

[121] K. Redlich and L. Turko, Phase transitions in the statistical bootstrap model with an internal symmetry, Z. Phys. C **5**, 201 (1980).

[122] F. Becattini, J. Cleymans, A. Keranen, E. Suhonen, and K. Redlich, Features of particle multiplicities and strangeness production in central heavy ion collisions between 1.7A and 158A GeV$/c$, Phys. Rev. C **64**, 024901 (2001).

[123] R. Averbeck, R. Holzmann, V. Metag, and R. S. Simon, Neutral pions and η mesons as probes of the hadronic fireball in nucleus-nucleus collisions around 1A GeV, Phys. Rev. C **67**, 024903 (2003).

[124] L. Bravina, A. Faessler, C. Fuchs, Z. D. Lu, and E. E. Zabrodin, Violation of energy per hadron scaling in a resonance matter, Phys. Rev. C **66**, 014906 (2002).

[125] J. Adams *et al.* (STAR Collaboration), Experimental and theoretical challenges in the search for the quark gluon plasma: The STAR Collaboration's critical assessment of the evidence from RHIC collisions, Nucl. Phys. **A757**, 102 (2005).

[126] W. Florkowski, W. Broniowski, and M. Michalec, Thermal analysis of particle ratios and p_T spectra at RHIC, Acta Phys. Pol. B **33**, 761 (2002).

[127] A. Baran, W. Broniowski, and W. Florkowski, Description of the particle ratios and transverse momentum spectra for various centralities at RHIC in a single-freeze-out model, Acta Phys. Pol. B **35**, 779 (2004).

[128] A. Cillis and S. J. Sciutto, Air showers and geomagnetic field, J. Phys. G **26**, 309 (2000).

[129] J. Knapp, D. Heck, S. J. Sciutto, M. T. Dova, and M. Risse, Extensive air shower simulations at the highest energies, Astropart. Phys. **19**, 77 (2003).